Project funded by the European Commission under the 6th (EC) RTD Framework Programme (2002- 2006) within the framework of the specific research and technological development programme "Integrating and strengthening the European Research Area"

Project UpWind

Contract No.:
019945 (SES6)

"Integrated Wind Turbine Design"

2nd order evaluation aerodynamic concept 1

Deliverable 1B3.6 & 7

AUTHOR:	Thanasis Barlas
AFFILIATION:	Delft University of Technology - DUWIND
ADDRESS:	Kluyverweg 1, 2629 HS, Delft, The Netherlands
TEL.:	+31 15 2785236
EMAIL:	a.barlas@tudelft.nl
FURTHER AUTHORS:	
REVIEWER:	
APPROVER:	

DOCUMENT TYPE	Deliverable Report
DOCUMENT NAME:	2nd order evaluation aerodynamic concept 1
REVISION:	
REV.DATE:	
CLASSIFICATION:	R1: Restricted to project members
STATUS:	

Contents

1. Introduction

This report summarizes the findings of Upwind WP 1B3 related with the evaluation of a chosen smart rotor control concept. The concept was chosen based on the preliminary findings of WP 1B3 (see deliverables 1B3.1, 1B3.3 and 1B3.4). It comprises a straightforward solution of using plain trailing edge flaps in an individual way (one big flap per blade) or a distributed way (multiple flaps per blade). In previous work, plain and flexible flap concepts were aerodynamically evaluated with 2d unsteady aerodynamic models (see deliverable 1B3.2). The concept now is evaluated more realistically using a dedicated aeroelastic tool (DU_SWAMP), simulating the integration and control of flaps on a full wind turbine configuration. Variations of the concept and control design methods are evaluated.
Due to the fact that, in the course of the project, there was no other aerodynamic concept that was mature enough to be evaluated in an aeroelastic environment, only this concept was tested. Thus, at this point, deliverable 1B3.7 is considered irrelevant and will not be pursued.

2. Numerical model

2.1 Model description

A comprehensive aeroservoelastic tool has recently been developed by researchers at Delft University Wind Energy Research Institute (DUWIND). Although a variety of widely used aeroelastic codes is available for design, certification and research purposes, the new code has been developed in order to have the advantage of a modular structure, to be able to incorporate realistic effects of distributed trailing edge flaps and to allow for rapid and easy design and implementation of real time controllers. These goals led to the development of DU_SWAMP (Delft University Smart Wind turbine Aeroelastic Modular Processing).

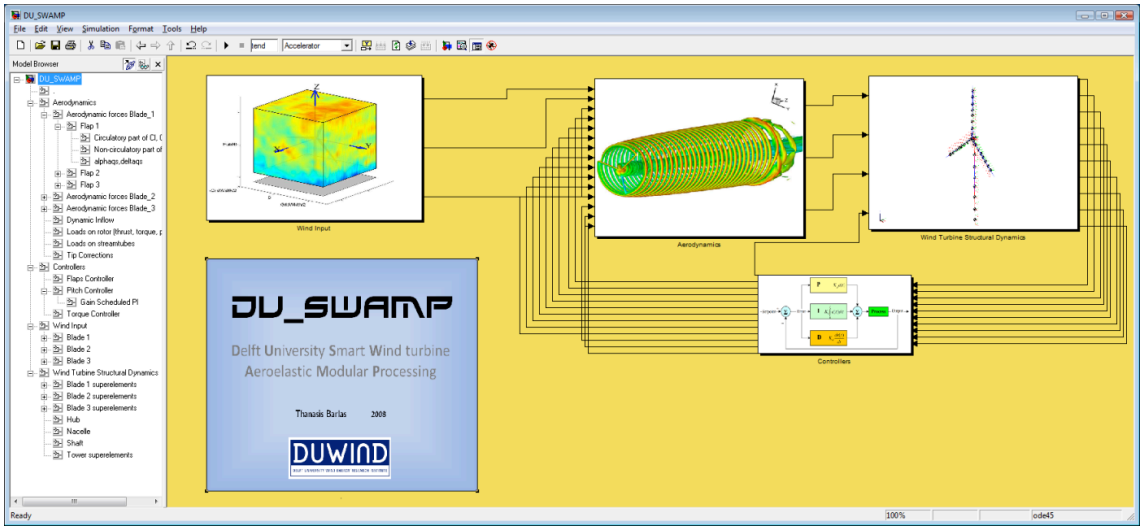

Figure 1: Simulink graphical interface showing sub-moules of the DU_SWAMP code.

The code is implemented in Matlab and Simulink and comprises a full aeroservoelastic wind turbine model, extended with distributed active control capability features. The structure of the code is fully modular, which offers the possibility to easily adapt the model configuration and complexity by interchanging modules at any level, as partly illustrated in Figure 1. The implementation of additional features like trailing edge flap aerodynamics models or actuator dynamics behaviour is thus facilitated. The model layout also offers the opportunity to use

model linearization, system identification and various controller design tools utilizing any available signal in the model. Innovative feedback or feed-forward control schemes based on single-input-single-output (SISO) or multiple-input-multiple-output (MIMO) schemes are easily implemented in DU_SWAMP.

The rotor aerodynamics submodel consists of a multiple-streamtube blade element representation coupled with a dynamic inflow model, as described by Snel [1] for the unsteady wake induction. The sectional aerodynamics are described by 2D tabulated data, corrected for 3D effects using the Viterna method [13,14]. For the case of the flapped sections, a 2D unsteady aerodynamic model is used. The unsteady flaps model is based on work for helicopters as described by Leishman [2,3]. The model analytically predicts the aerodynamic responses of a thin airfoil to arbitrary forcing inputs (airfoil motion, gusts, flap deflection) through an indicial response formulation. Thus, the dynamic effect of a flap actuation is realistically simulated. In fact, the analytical state-space solution is a time-domain representation of the Theodorsen and Wagner function (see Theodorsen [4], Wagner [5], and Bisplinghoff [6]). The model is valid for attached flow conditions. The model has been adapted for wind turbine applications. The general theoretical background is explained with more detail in Reference [11]. The model superimposes unsteady effects due to angle of attack changes, wind gusts, and flap actuations.

The aeroelastic model is modified for this work such that the NREL TurbSim [12] code could be used to generate 3D turbulent inflow as input to the DU_SWAMP simulations. This feature allows direct comparisons of system responses to the same inflow by both DU_SWAMP and other widely used codes, like FAST and BLADED. All three components of the variable wind velocity are utilized by the DU_SWAMP aerodynamic models.

The structural dynamics sub-model of the wind turbine is aeroelastically coupled to the aerodynamic model, by means of the structural deformation velocities and the aerodynamic forces. This sub-model consists of a hybrid multibody representation of the wind turbine components. The main flexible structural components (i.e. blades and tower) are represented by superelements (i.e. sets of non-equally distributed rigid bodies connected with linear springs and dampers, see Figure 2). These are connected with other rigid bodies to formulate the full wind turbine multibody structural problem. All necessary blade degrees of freedom are included (flap-wise bending, edgewise bending and torsion, if chosen). The total number of degrees of freedom in the full wind turbine configuration is determined by the number of superelements used per flexible body. In order to capture the first two bending modes of blades and tower, two to three superelements are used. This leads to 40 to 60 degrees of freedom in the full wind turbine configuration.

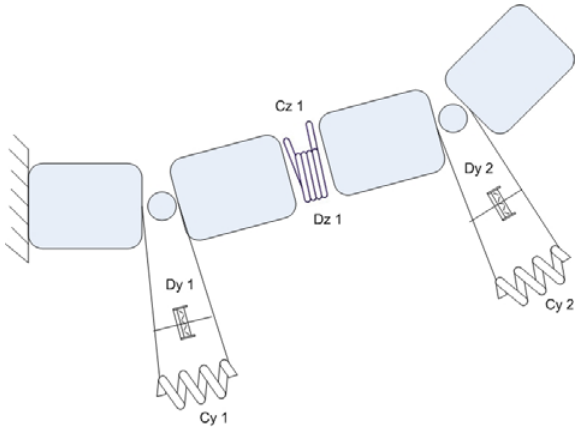

Figure 2: Superelement multi-body representation.

The baseline controllers of the wind turbine are included for power regulation, i.e. generator torque control and above rated full-span pitch control. Any addition of other kinds of load reduction controller, like cyclic or individual pitch control, individual flap control (one flap per

blade), or distributed flap control is facilitated. Virtually any signal can be used for controller input. The actuator dynamics can also be specified in detail, by means of transfer functions, low order dynamic systems, or by setting saturation limits and rate limits for the actuation. This allows for detailed modeling of smart-material based actuation, which has an important impact on the dynamics of the full model.

2.2 Model verification

Sandia National Laboratories and TU-Delft have worked together to verify the DU_SWAMP code against FAST [15]. FAST [17] is chosen as a verification code not because it is believed to represent reality, but because it represents a code that has been used for several active aerodynamic control studies in the past.
Both steady and turbulent wind input cases are used in the comparisons. Initial verifications serve to emphasize the benefits and shortcomings of the simulation capabilities for each model. Initial model comparisons are performed over the full operational range of the turbine.
Steady state system response is computed for steady wind speeds at increments of 2 m/s from 5 to 23 m/s. Selected steady wind comparisons are shown in Figure 3.

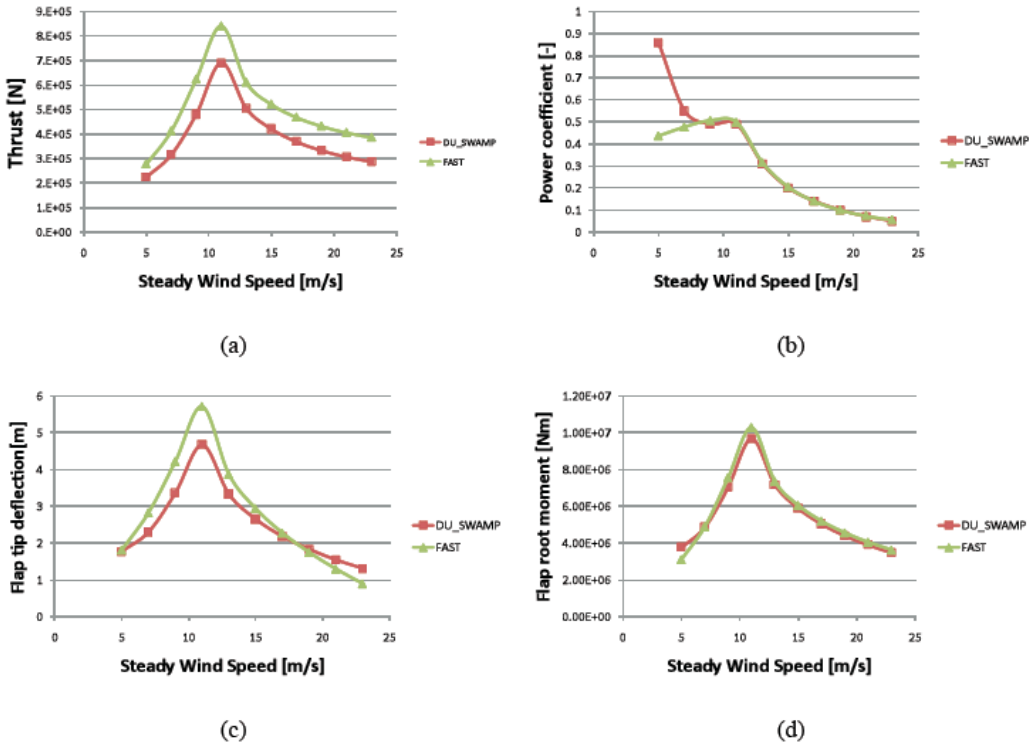

Figure 3: Comparison of steady-state model response to constant wind input (DU_SWAMP vs. FAST).

It is seen that FAST over-predicts thrust values due to the different dynamic inflow model used. Moreover, the empirical corrections of DU_SWAMP for high thrust coefficient break down for very low wind speeds. General agreement in steady-state conditions is good.

The next step in model verification compares dynamic response of the models when a three-dimensional full-field turbulent wind input is supplied. The three-dimensional wind input is generated by TurbSim with 6% turbulence intensity, generated according to the Kaimal spectrum. For consistency, the same wind input files are used to excite both the DU_SWAMP model and the FAST model. Four models are compared. FAST/AeroDyn results are shown for

both the BEM model and the GDW model. DU_SWAMP results are shown for two different implementations of aerodynamic modules. One model, designated Vinf_average, assumes a constant estimate of hub height wind speed in the calculation of streamtube loads, dynamic inflow, rotor loads, and tip corrections. The other model, designated Vinf_instantaneous, assumes a time-varying estimate of the wind speed at hub height in the same calculations. Selected turbulent wind comparisons are shown in Figure 4.

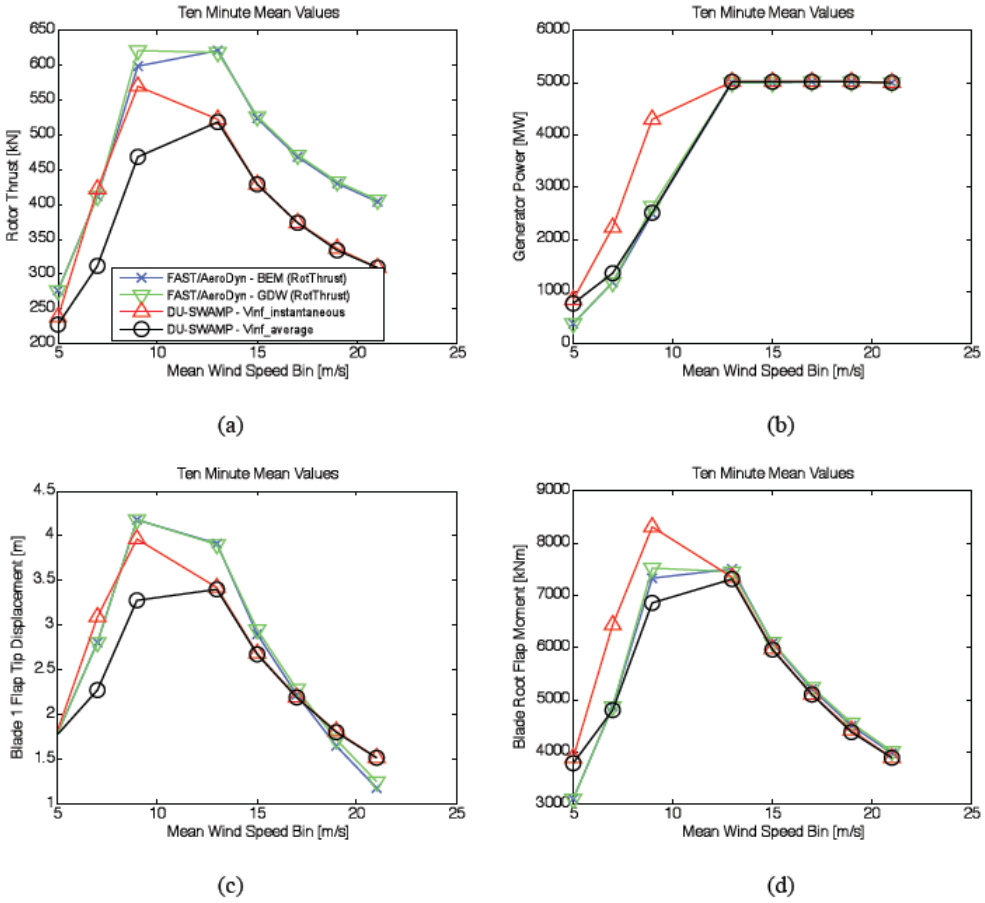

Figure 4: Comparison of model response to turbulent wind input (DU_SWAMP vs. FAST).

Results show similar trend as in the steady-state response. The implementation of the average wind speed in DU_SWAMP's aerodynamic modules seems to produce more consistent results. Generally, agreement in turbulent conditions is good.

3. Results

The Upwind/NREL 5MW reference wind turbine is used as a baseline for all simulations. In the first part of the presented results, flap control concepts are shown and compared, using simplified classical controller design approaches [11]. In the second part, more advanced controller design implementation is utilized [15,16].

3.1 Simple control design

Three main global load control strategies are considered and are investigated:

- *Decentralized individual flap control*
  One large flap per blade is used. Each flap reacts on the same blade's flapping root moment based on a feedback control rule. All three single-input-single-output (SISO) feedback loops are decoupled, thus this control scheme is referred to as decentralized

- *Centralized individual flap control*
  One large flap per blade is used. A multi-blade rotational transformation technique is used to transform blade root flapping moments into rotor yaw and tilt moments. This results in two decoupled SISO feedback loops. A third SISO loop can be used to impose a collective flap angle, used additionally for power regulation. Since the three individual flaps are control based on global rotor signals (in fixed reference frame), this control scheme is referred to as centralized.

- *Decentralized multiple feedback flap control*

Multiple flaps per blade are used. Each flap is activated based on local flapwise deformation signals via a feedback rule. All SISO loops are fully decoupled.

For every case, representative operating wind speeds are chosen (8, 11.4 and 16 m/s), covering below and above rated wind speed operation. The baseline controllers for power regulation (i.e. generator torque control and above rated collective pitch) are used normally in every case. The linearized models are computed around each relevant operating point, in an averaged way, in order to eliminate periodic effects. The models obtained are analyzed in terms of frequency response, and a PID controller is designed using classical control methods with the target of minimizing the fluctuations in the required signal in every case (blade root flapwise bending moment, local deflections). Additional highpass and lowpass filters are also used in order to use only the dynamic part of the sensor signals and suppress unwanted high frequencies, respectively.

The concepts are compared in terms of fatigue load reduction performance, primarily quantified with the standard deviation of flapwise blade root bending moment. Every case is analyzed in order to determine the physical basis that drives the differences in performance. Conclusions are drawn about the optimization of the integration of active flaps on wind turbine blades, considering realistic design options.
In the Individual Flap Control cases, one big flap of 20% blade spanwise length is used. The flaps occupy 10% of the chordwise length in every used section. The allowed flap angles (saturation limits) are ±10 degrees and the maximum flap rate is ±40 degrees per second, corresponding to realistic performance of actuators based on smart materials or compliant mechanism structures. In the Multiple Flap Control case, the same area of flap is used (20%R), split into three parts. Local flapwise deformation signals are used as inputs to the controller. The main results from the IEC standard power production normal turbulence load cases can be seen below.
The time series results from the decentralized IFC are shown in Figure 5. We see the activity of each flap on every blade using the designed feedback control law based on each blade's flapwise root moment. A considerable reduction in both the standard deviation of the flapwise root moment and flapwise tip deflection is achieved. The perodicity of the system, especially around the rotor frequency (1p) can be seen together with the appropriate flap response.

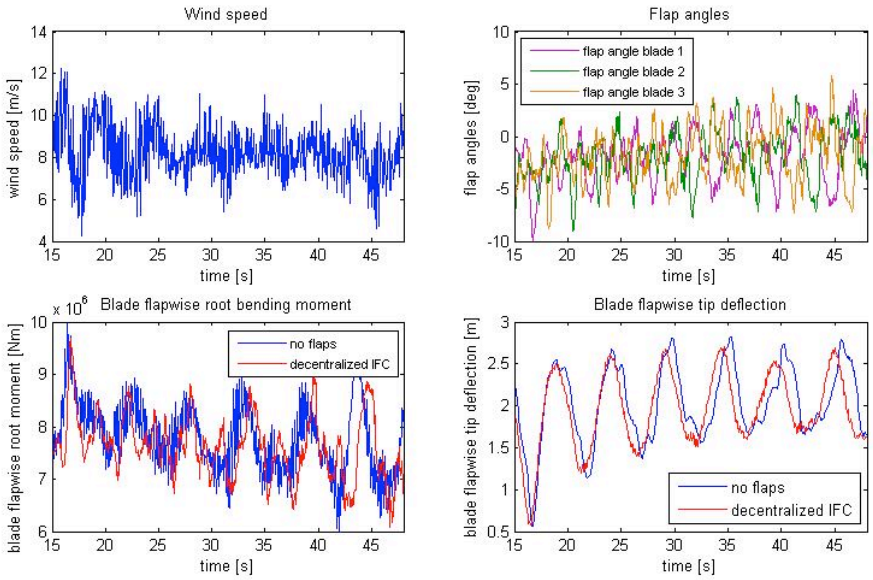

Figure 5: Time series with Decentralized Individual Flap Control.

The time series results from the centralized IFC are shown in Figure 6. In this case, the flaps react based on the designed feedback control law, in order to alleviate fluctuations in the rotor tilt and yaw moments. A considerable reduction in both the standard deviation of the flapwise root moment and flapwise tip deflection is achieved.

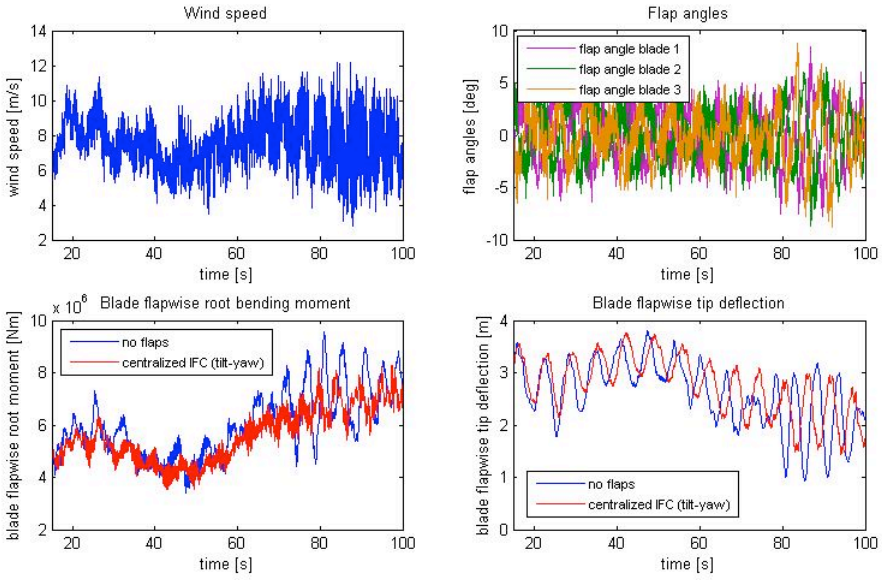

Figure 6: Time series with Centrialized Individual Flap Control (Coleman or 'tilt-yaw').

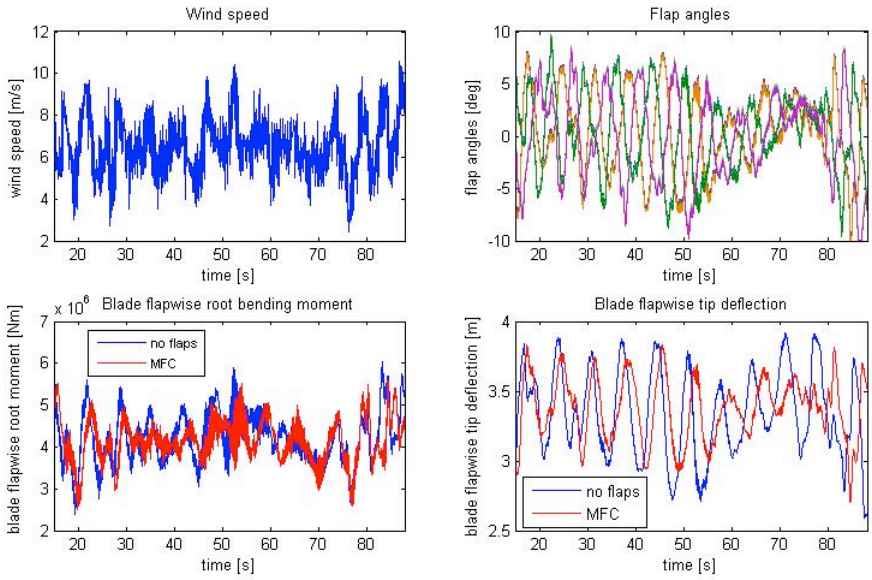

Figure 7: Time series with Decentralized Multiple Flap Control.

The time series results from the decentralized MFC are shown in Figure 7. In this case, the three flaps per blade react independently based on the designed feedback control law, in order to alleviate fluctuations in the local flapwise deformations. A considerable reduction in both the standard deviation of the flapwise root moment and flapwise tip deflection is achieved.
In all the cases, a reduction in the standard deviation of the collective pitch angle was also achieved, since the reduction in fluctuating loads at low frequencies also helps in regulating the rotor speed. On the other hand, a slight decrease in mean power was observed, something that has been discussed also in other relevant publications [11,22]. No particular effort has been put in modifying the control law to compensate for that, although the possibility has been verified. Results for all investigated load cases are compiled in Table 1.

Table 1: Results for all load cases 9 (% reduction).

control scheme		**IFC**			**IFC-Coleman**			**MFC**	
average wind speed	8 m/s	11.4 m/s	18 m/s	8 m/s	11.4 m/s	18 m/s	8 m/s	11.4 m/s	18 m/s
flap root moment std	15.41	10.23	17.32	9.26	5.78	7.92	19.32	16.35	22.41
flap tip deflection std	9.26	5.54	10.21	8.01	2.61	1.91	31.01	20.54	34.52
FA tower root moment	4.31	3.67	5.01	3.47	8.99	1.47	17.25	15.56	18.33
FA tower top deflection	3.98	3.02	4.13	4.49	9.24	0.97	15.93	13.21	16.02
Mean generator power	-0.89	-0.53	-0.45	-1.22	-0.32	-0.14	-0.88	-0.61	-0.54
Pitch angle std	-	9.27	10.03	-	10.57	12.25	-	8.32	10.16

Comparing all results for the different load cases and control schemes, it can be seen that decentralizing the control loops has a positive effect on the load reduction potential. This is explained due to the large deviations in time and space of the local disturbances and their responses. More detailed load control can be achieved by distributing the control capability. The control design is not necessarily more complicated as soon as no strong couplings are present between the individual loops.

3.2 Advanced control design

Additional simulations utilizing DU_SWAMP and FAST have been performed, using more dedicated controller design methods. Two types of closed loop control schemes are used in the demonstration: 1) a PD style controller and 2) a high pass filter, to remove the static loads, combined with an inverted notch at the 1P frequency to target the dominant energy in the load spectrum. These simulations employ one flap per blade.
Schematics of the two approaches are shown in Figure 1. The objective of the controller is to minimize fluctuations of the blade flapwise tip displacements and, indirectly, blade root loads. The PD controller was exactly replicated in both DU_SWAMP and FAST/Simulink in order to gain an understanding of the differences due to structural representations and aerodynamic flap models. The inverted notch controller is demonstrated only in DU_SWAMP. Controllers are designed based on linear models obtained using system identification techniques.
Results shown below utilize the DU_SWAMP model with average estimate of hub height wind speed, Vinf_average. The wind input used in the comparison of active aero control is, as stated above, three dimensional full field turbulent winds with 6% turbulence intensity. A single wind condition in the lower portion of Region 3 at 15 m/s was chosen for the demonstration of active flap control. Time-series of results can be seen in Figure 9.

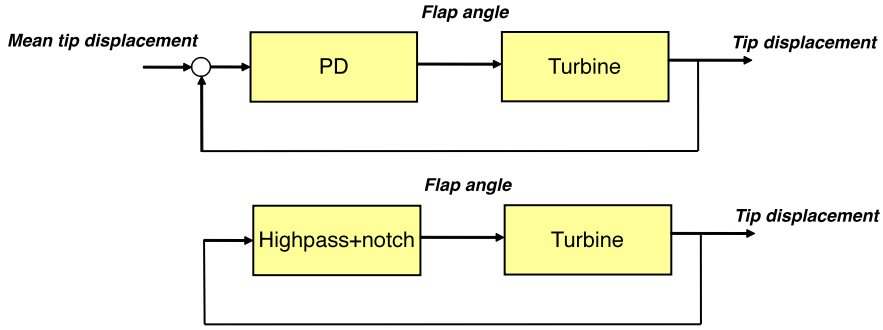

Figure 8: Schematics of the two control approaches

The simulation responses are used in a simple fatigue loads analysis in order to arrive at a final estimate of damage equivalent load reductions. Flapwise root moments are rain flow counted by NREL's Crunch, and results are processed to yield damage equivalent load ratios.

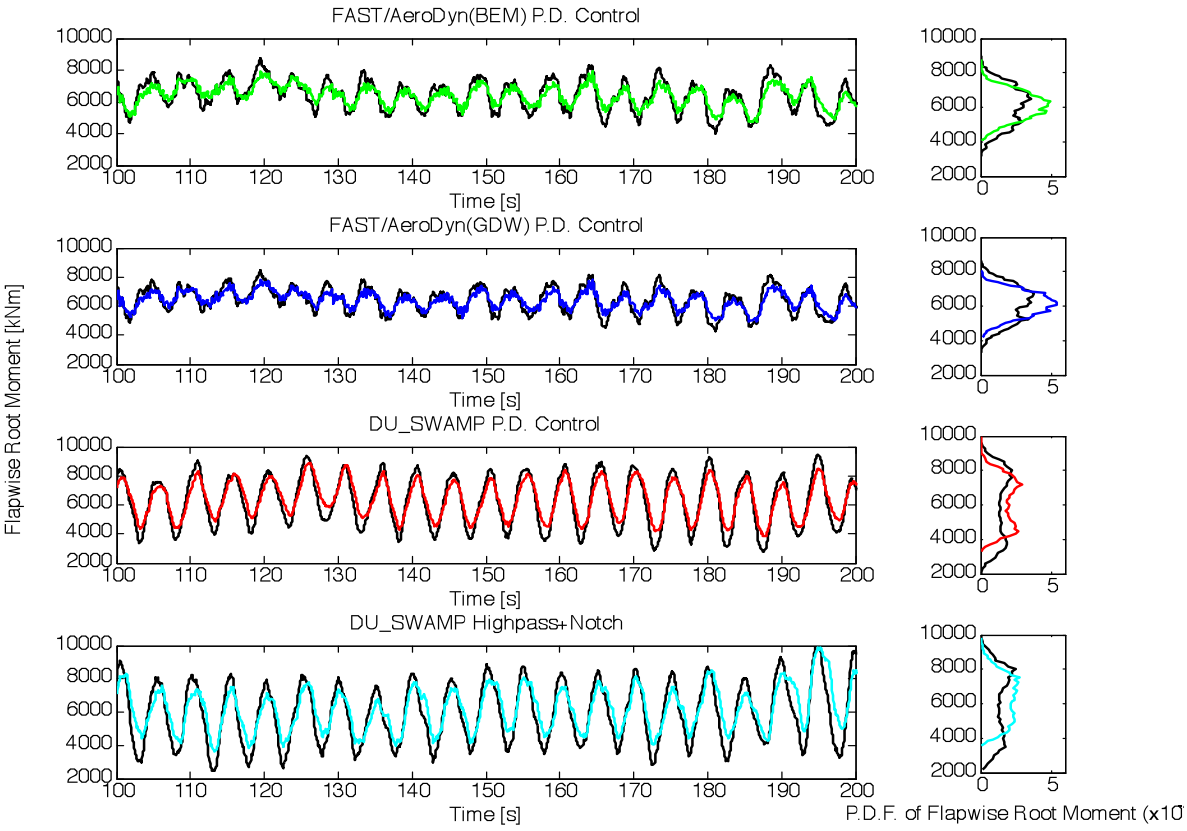

Figure 9: Time domain comparison of baseline responses (black) to responses with active aero PD control (red,blue,green) and highpass filter with inverted notch (cyan)

Table 2 summarizes load reductions due to active aero control. Reductions in both time waveform standard deviation and damage equivalent load (DEL) are shown. Damage equivalent load reductions are computed for material fatigue exponents of 3 and 10, representing steel and fiberglass, respectively. There is little difference between the two FAST models. The fatigue load reduction benefits for all the cases are similar.

Table 2: Damage equivalent load reductions in blade flapwise root moment.

Model Type	Percent reduction in waveform standard deviation, flapwise root moment, 15 m/s	Percent Reduction in DEL, 15 m/s Fatigue exponent, b	
		b = 10 glass composite	b = 3 steel
FAST/AeroDyn with GDW, PD	30.9 %	30.5 %	33.2 %
FAST/AeroDyn with BEM, PD	29.2 %	31.3 %	34.6 %
DU_SWAMP, PD Controller	26.0 %	29.3 %	30.2 %
DU_SWAMP, Highpass+Notch	30.1 %	27.0 %	31.6 %

In an additional simulation effort, distributed control system design is performed for multiple flaps per blade. The DU_SWAMP model is again utilized.
This time, the Observer/Kalman filter IDentification (OKID) method is used to extract a linear model of the system from DU_SWAMP data. The system is excited with chirp signals at individual flaps and the output is measured. The corresponding observer match with actual responses of the non-linear DU_SWAMP signals.
The controller was designed using standard LQR methodology using the identified state estimator from the OKID algorithm. The results show a 15.5 % reduction in fatigue damage equivalent load and a 13.3% reduction in the standard deviation of the waveform. Time-series of flapwise moment and tip deflection with and without flaps control are shown in Figure 10. The flaps activity, showing the distributed nature of the actuation signal, per blade and per flap location, is shown in Figure 11.

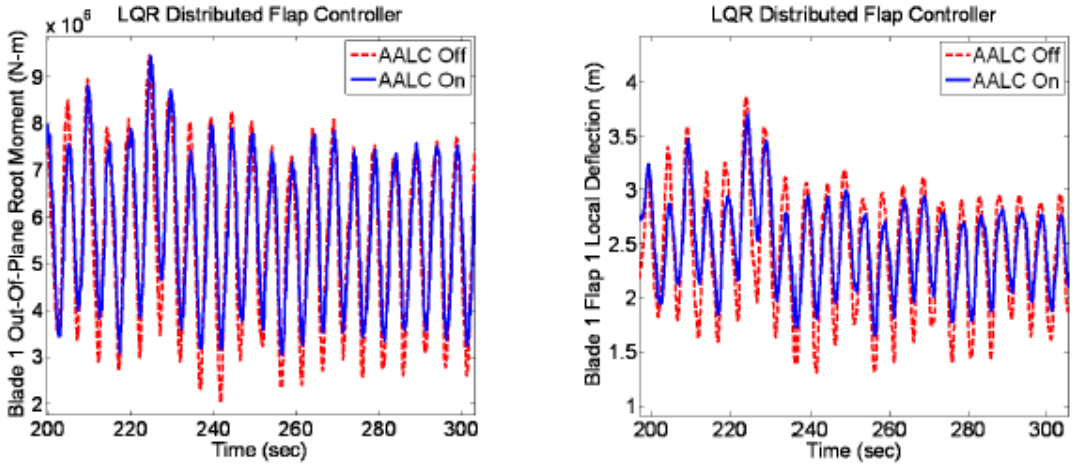

Figure 10: Blade 1 out-of-plane root moment response (left) and local deflection response (right) both with and without LQR flap controls.

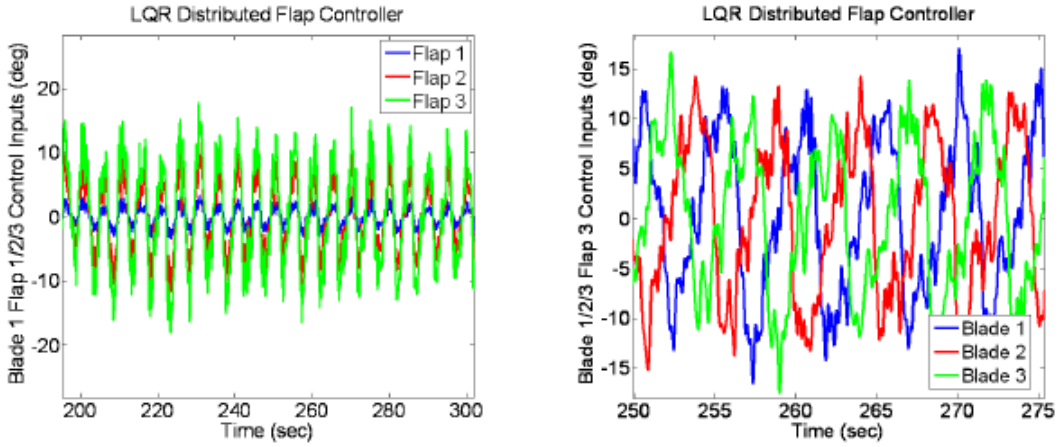

Figure 11: LQR controller input flaps 1,2,3 and blade 1,2,3 flap 3 (right) inputs.

4. Conclusions

This report summarizes the findings of Upwind WP 1B3 related with the evaluation of a chosen smart rotor control concept, namely integrated rigid trailing edge flaps along the span of the blades. The dedicated aeroservoelastic tool DU_SWAMO was utilized for this analysis. The tool was verified against traditional aeroelastic codes and the flap concept was simulated. A range of implementation of the concept has been tested numerically: Individual or distributed flaps per blade, different sensor choices, different controller schemes. Results show that using more advanced controller schemes and distributing the flaps can increase the expected load reduction potential. More work in the future can focus on optimizing the smart rotor design with the specific concept. Issues like flaps placement, flaps geometry, type and placement of sensors and optimal blade design for flaps are necessary for future implementation of this concept.

5. References

[1] Snel H. Survey of induction dynamics modelling within BEM-like codes: Dynamic inflow and yawed flow modelling revisited. *Proceedings of the 39th AIAA/ASME*, Reno, NV, USA, 2001.
[2] Leishman J G. Unsteady lift of a flapped airfoil by indicial concepts. *Journal of Aircraft* 1994; 31: 288-297
[3] Leishman J G. *Principles of helicopter aerodynamics*, 2nd edition, Cambridge aerospace series, 2006.
[4] Theodorsen T. General theory of aerodynamic instability and the mechanism of flutter. *NACA Technical Report 497*, 1935.
[5] Wagner H. Über die entsehung des dynamischer auftriebes von tragflügeln. *Z. Angew. Math. U. Mech*., Vol. 118, 1982; 393-409.
[6] Bisplinghoff R L, Ashley H, Halfman R L. *Aeroelasticity*. Addison-Wesley Publishing Co.,1955.
[7] Molennar D-P. Cost-*effective design and operation of variable speed wind turbines*, PhD Thesis. Delft University Press, 2003.
[8] Holierhoek J G. Aeroelasticity of large wind turbines. PhD Thesis. Delft University Press, 2008.
[9] Shabana A A. Flexible multibody dynamics: Review of past and recent developments. *Multibody system* dynamics 2001; 1: 189-222.
[10] Rauh J, Schiehlen W. Various approaches for the modeling of flexible robot arms. *Proceedings of the Euromech-Colloquium 219 on refined dynamical theories of beams, plates and shells and their applications*.1987; 420-429.
[11] Barlas, T.K., and van Kuik, G.A.M., "Aeroelastic Modelling and Comparison of Advanced Active Flap Control Concepts for Load Reduction on the Upwind 5MW Wind Turbine". European Wind Energy Conference, Marseille, France, 16-19 March, 2009.
[12] NWTC Design Codes (TurbSim by Neil Kelley and Bonnie Jonkman), http://wind.nrel.gov/designcodes/preprocessors/turbsim/.
[13] NWTC Design Codes (AirfoilPrep by Dr. Craig Hansen).
http://wind.nrel.gov/designcodes/preprocessors/airfoilprep/. Last modified 16-January-2007; accessed 16-January-2007.
[14] Viterna, L.A. and Corrigan, R.D., "Fixed Pitch Rotor Performance of Large Horizontal-Axis Wind Turbines", Proceedings of a Workshop on Large Horizontal-Axis Wind Turbines Held in Cleveland, Ohio, July 28-30, 1981, Robert Thresher, Editor, SERI/CP-635-1273 (DOE Publication CONF-810752, NASA Conference Publication 2230). 1982, pp. 69-85.

[15] Resor, B., Wilson, D., Berg, D., Berg, J. , Barlas, T., and van Kuik, G., “The Impact of Higher Fidelity Models on Active Aerodynamic Load Control Fatigue Damage Reduction”, *Proceedings of the 48th AIAA Aerospace Sciences Meeting*, Orlando, FL, January 4-7, 2010.
[16] Wilson, D.G., Resor, B.R, Berg, D.E., Barlas, T.K., and van Kuik, G.A.M., “Active Aerodynamic Blade Distributed Flap Control Design Procedure for Load Reduction on the UpWind 5MW Wind Turbine,” *Proceedings of the 48th AIAA Aerospace Sciences Meeting*, Orlando, FL, January 4-7, 2010.
[17] NWTC Design Codes (FAST by Jason Jonkman), http://wind.nrel.gov/designcodes/simulators/fast/.
[18] NWTC Design Codes (Crunch by Marshall Buhl). http://wind.nrel.gov/designcodes/postprocessors/crunch/.